Electronic structure and optical properties of $Mg_xZn_{1-x}S$ bulk crystal using first-principles calculations*

Yu Zhi-Qiang(余志强), Xu Zhi-Mou(徐智谋)†, and Wu Xing-Hui(武兴会)

Wuhan National Laboratory for Optoelectronics, School of Optical and Electronic Information, Huazhong University of Science and Technology, Wuhan 430074, *China*

(Received 10 March 2014; revised manuscript received 21 April 2014; published online 20 August 2014)

We perform the first-principles calculations within the framework of density functional theory to determine the electronic structure and optical properties of $Mg_xZn_{1-x}S$ bulk crystal. The results indicate that the electronic structure and optical properties of $Mg_xZn_{1-x}S$ bulk crystal are sensitive to the Mg impurity composition. In particular, the $Mg_xZn_{1-x}S$ bulk crystal displays a direct band structure and the band gap increases from 2.05 eV to 2.91 eV with Mg dopant composition value x increasing from 0 to 0.024. The S 3p electrons dominate the top of valence band, while the Zn 4s electrons and Zn 3p electrons occupy the bottom of conduction band in $Mg_xZn_{1-x}S$ bulk crystal. Moreover, the dielectric constant decreases and the optical absorption peak obviously has a blue shift. The calculated results provide important theoretical guidance for the applications of $Mg_xZn_{1-x}S$ bulk crystal in optical detectors.

Keywords: first-principles, $Mg_xZn_{1-x}S$, electronic structure, optical properties

PACS: 71.20.–b, 78.20.Ci **DOI:** 10.1088/1674-1056/23/10/107102

1. Introduction

II–VI semiconductors, each with a high light emitting efficiency and large direct band structure at room temperature, have received considerable attention.[1] Moreover, II–VI semiconductors are found to have potential applications in optical wave guides, visible light emitting devices, blue laser, optical devices, etc.[2] As one of the important II–VI semiconductors, zinc-blende ZnS with a wide direct band gap value of 3.72 eV[3] has attracted considerable attention, owing to its broad potential applications in lasers, light emitting diodes, electroluminescent devices, fluorescent probes, optoelectronic devices, and optical coatings.[4–7]

In recent years, many people have found that the band structure of pure ZnS can be effectively modified by introducing some impurities or defects. Hoa *et al.*[8] have found that the band structure of ZnS nanocluster changed with Mn impurity concentration. Kim *et al.*[9] have reported that the band structure of Te-doped ZnS nanowire reduced from 3.21 eV to 2.78 eV, corresponding to a dopant composition range from 0 to 0.22. Inoue *et al.*[10] have presented that the optical band gap energy (E_g) of $Zn_xMg_{1-x}S$ thin film can be evaluated by the first order equation $E_g = 3.81x + 5.02(1-x)$, with concentration x being between 0.14 and 1. Chen *et al.*[11] have experimentally shown that the PL intensity weakens and the band gap of $Mg_xZn_{1-x}S$ quantum dots increase with increasing Mg concentration. However, theoretical investigation on the electronic structure and optical properties of $Mg_xZn_{1-x}S$ bulk crystal are still lacking.

In this paper, we perform the first-principles calculations within the framework of density functional theory to investigate the electronic structure and optical properties of $Mg_xZn_{1-x}S$ bulk crystal. The results show that the electronic structure and optical properties are sensitive to the Mg impurity composition in $Mg_xZn_{1-x}S$ bulk crystal. The effects of Mg composition on the band structure, density of states, and optical properties of zinc-blende ZnS are obtained in detail. The results provide useful theoretical guidance for the applications of $Mg_xZn_{1-x}S$ bulk crystal in optical detectors.

2. Models and method

The zinc-blende ZnS has a space group of F-43m,[12] and the pure ZnS bulk crystal with $1\times1\times1$ unit cell is shown in Fig. 1. The $Mg_xZn_{1-x}S$ bulk crystal can be displayed by substituting the Zn atoms by Mg atoms, and the $Mg_xZn_{1-x}S$ bulk crystal model is constructed in the framework of $4\times4\times2$ supercell. We employ one, two, and three Mg atoms to replace Zn atoms in the $4\times4\times2$ supercell, thus the values of dopant composition x correspond to 0.008, 0.016, and 0.024, respectively. The crystal structure of $Mg_xZn_{1-x}S$ bulk crystal is isomorphic with the pure ZnS bulk crystal owing to the substitutive doping.

The first-principles calculations based on the density functional theory[13] are implemented by using the Cambridge Sequential Total Energy Package[14] (CASTEP) code, and the generalized gradient approximation[15] (GGA) is used for the exchange correlation function in the framework of Perdew–Burke–Ernzerhof[16] (PBE). The Brillouin zone integrations with $5\times5\times5$ k-point meshes and $4\times4\times4$ k-point meshes

*Projected supported by the National Natural Science Foundation of China (Grant Nos. 61076042 and 61474048).

†Corresponding author. E-mail: xuzhimou@hust.edu.cn

© 2014 Chinese Physical Society and IOP Publishing Ltd

are performed in the form of Monkhorst–Pack scheme for the pure and Mg-doped ZnS bulk crystal, respectively. The convergence criterion for the plane wave energy cutoff is set to be 310 eV. The convergence accuracy for the maximal force between the atoms is 0.02 eV/Å and the self-consistent convergence criterion is 1.8×10^{-7} eV/atom. In addition, the $3d^{10}4s^2$, $3s^23p^4$, and $2p^63s^2$ electrons relevant to the Zn, S, and Mg atoms are used for the pseudopotential configurations, respectively.

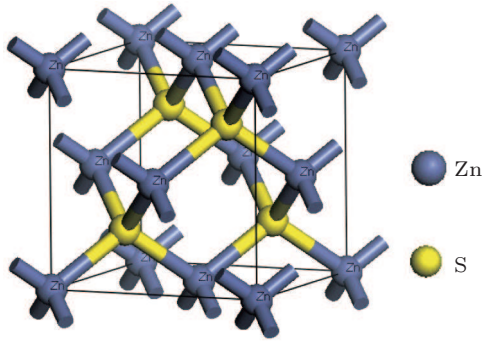


Fig. 1. (color online) Crystal structure of pure ZnS unit cell.

3. Results and discussion

3.1. Geometry optimization results

The optimized lattice parameters and total energies of pure and Mg-doped ZnS bulk crystals are shown in Table 1. It is clear that the optimized lattice parameter of pure ZnS bulk crystal, 0.5467 nm, is in good agreement with the experimental lattice parameter of 0.5416 nm,[17] within an error of around 0.9%, and the lattice constants of $Mg_xZn_{1-x}S$ bulk crystal increase with the increase of Mg doping concentration, which relates to the increase of bond length d_{Zn-S} between Zn and S atoms and the smaller electronegativity of Mg atom than that of Zn atom. In particular, the total energy of $Mg_xZn_{1-x}S$ bulk crystal first decreases and then increases, which shows that the system stability of $Mg_xZn_{1-x}S$ bulk crystal increases according to the lowest energy principles. Meanwhile, the most possible substitution location of $Mg_xZn_{1-x}S$ bulk crystal is presented in $Mg_{0.008}Zn_{0.992}S$ when considering the system's stability.

Table 1. Optimized lattice parameters and total energies of $Mg_xZn_{1-x}S$ bulk crystal (x at 0, 0.008, 0.016, and 0.024).

Models	$a=b=c$/nm	d_{Zn-S}/nm	E/eV
ZnS	0.5467	0.2366	–1989.35
$Mg_{0.008}Zn_{0.992}S$	0.5517	0.2368	–7222.96
$Mg_{0.016}Zn_{0.984}S$	0.5628	0.2376	–3244.14
$Mg_{0.024}Zn_{0.976}S$	0.5658	0.2384	–5753.62

3.2. Electronic structure

In order to understand the electronic structures of $Mg_xZn_{1-x}S$ bulk crystal. The density of states and band structures of $Mg_xZn_{1-x}S$ bulk crystal are determined, and the results are shown in Figs. 2–7, respectively. As shown in Fig. 2, the pure and Mg-doped ZnS bulk crystals display a direct band gap along the G–G direction in the first Brillouin zone, and the increase of the band gap of $Mg_xZn_{1-x}S$ bulk crystal with the increase of Mg dopant composition x. The band gap value of pure ZnS bulk crystal is 2.05 eV, which is close to the earlier

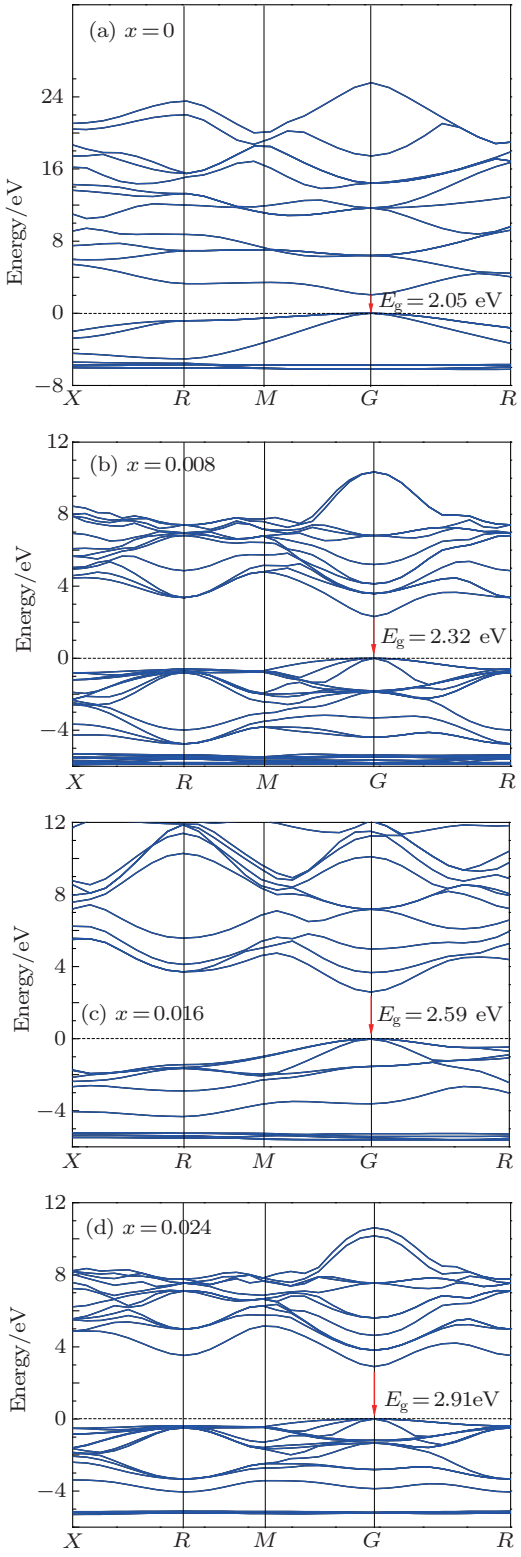


Fig. 2. (color online) Band structures of (a) pure ZnS, (b) $Mg_{0.008}Zn_{0.992}S$, (c) $Mg_{0.016}Zn_{0.984}S$, and (d) $Mg_{0.024}Zn_{0.976}S$.

band gap value of 2.17 eV.[18] However, the band gap value of 2.05 eV is lower than the experimental value of 3.77 eV,[19] owing to the limitation of density functional theory, which relates to the discontinuity of exchange correlation potential and has not been performed in the framework of density functional theory.

The band structures of $Mg_xZn_{1-x}S$ bulk crystal are shown in Figs. 2(a)–2(d), respectively. It is found that the band gap of $Mg_xZn_{1-x}S$ bulk crystal increases from 2.05 eV to 2.91 eV with the increase of Mg doping concentration x in a range from 0 to 0.024. In particular, the band gap (E_g) of $Mg_xZn_{1-x}S$ bulk crystal varies with the dopant concentration x, as displayed in Fig. 3, and it is observed that the band gap of $Mg_xZn_{1-x}S$ bulk crystal can be evaluated by the first order function $E_g = 2.05 + 35.62x$, where Mg dopant composition x in a range from 0 to 0.024. This clearly elucidates the linear relation between the band gap and dopant composition of $Mg_xZn_{1-x}S$ bulk crystal. Moreover, compared with the band gaps of two-dimensional $Zn_xMg_{1-x}S$ thin films[10] ranging from 3.81 eV to 3.84 eV with dopant composition x being between 1 and 0.976, the band gaps of three-dimensional $Mg_xZn_{1-x}S$ bulk crystal ranging from 2.05 eV to 2.91 eV corresponding to dopant composition x range from 0 to 0.024 are low, which may be induced by the quantum size effects of low-dimensional $Mg_xZn_{1-x}S$ nanostructures.

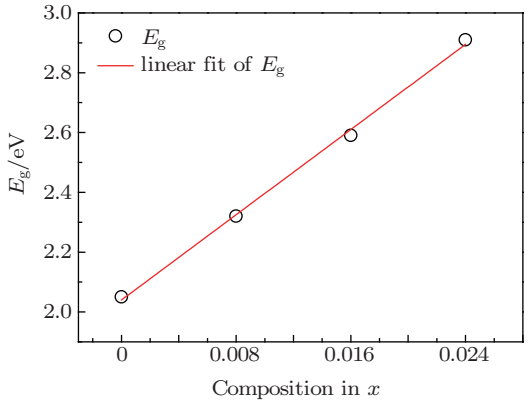


Fig. 3. (color online) Band gaps of $Mg_xZn_{1-x}S$ at $x = 0$, 0.008, 0.016, and 0.024.

In order to elucidate the electronic properties of $Mg_xZn_{1-x}S$ bulk crystal, the total density of states (TDOS) and partial density of states (PDOS) for pure ZnS bulk crystal are shown in Figs. 4(a)–4(c). It is observed that the valence band of pure ZnS bulk crystal is mainly divided into two regions. The lower energy region located around −12 eV is mainly dominated by the S 3s electrons, while the S 3p electrons, Zn 3p electrons and Zn 3d electrons occupy the higher energy range from −8 eV to 0 eV in the valence band. The conduction band above the Fermi surface is mainly composed of the Zn 4s electrons, Zn 3p electrons, and S 3p electrons. In addition, the valance band maximum (VBM) along the *G*–*G* direction is near the Fermi surface and it is mainly contributed by the S 3p electrons, while the conduction band minimum (CBM) along the *G*–*G* direction is 2.05 eV above the Fermi surface, and it is mainly determined by the Zn 4s electrons

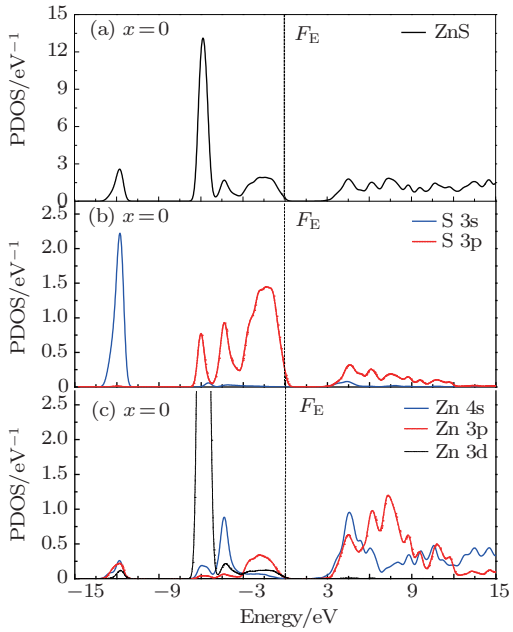


Fig. 4. (color online) Electronic densities of states for pure ZnS.

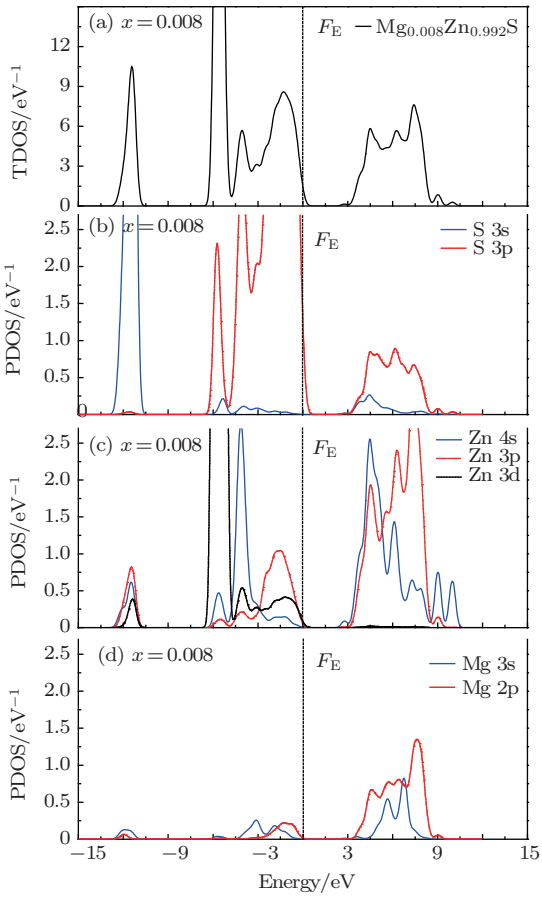


Fig. 5. (color online) Electronic densities of states for $Mg_{0.008}Zn_{0.992}S$.

and Zn 3p electrons, which construct the direct band structure of pure ZnS bulk crystal in Fig. 2(a).

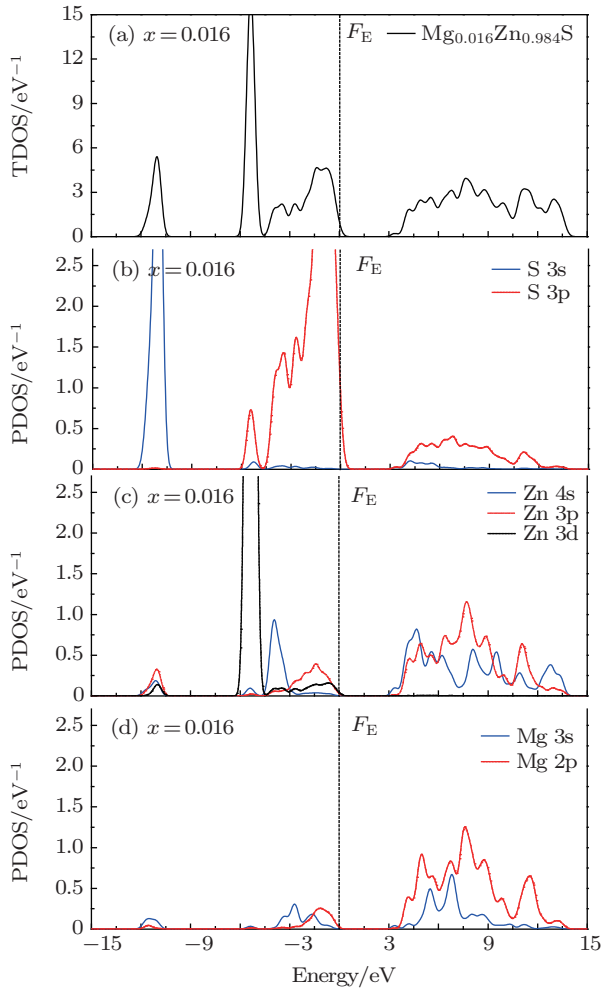


Fig. 6. (color online) Electronic densities of states for $Mg_{0.016}Zn_{0.984}S$.

The TDOS and PDOS of $Mg_xZn_{1-x}S$ bulk crystal are shown in Figs. 5–7, respectively. As shown in Figs. 5–7, the VBM along the *G*–*G* path that is near the Fermi surface is mainly occupied by the S 3p electrons, while the CBM along the *G*–*G* direction which is above the Fermi surface is mainly dominated by the Zn 4s electrons, Zn 3p electrons, and Mg 2p electrons in $Mg_xZn_{1-x}S$ bulk crystal. In particular, compared with the band gap of pure ZnS bulk crystal, the VBM along the *G*–*G* direction clearly shifts downwards to a lower energy region with the increase of Mg dopant concentration in $Mg_xZn_{1-x}S$ bulk crystal, which relates to the decrease of p–d type hybridization effects due to the deficiency of 3p electrons for Mg as compared with for Zn, and the p–p type hybridization effects of Mg 2p electrons with Zn 3p electrons. It is also observed that the CBM along the *G*–*G* path shifts upwards higher energy region with the increase of Mg dopant composition in $Mg_xZn_{1-x}S$ bulk crystal, while it results from the s–s type hybridization effects of Mg 2s electrons with Zn 4s electrons and S 3s electrons, which leads to the increase of band gap in $Mg_xZn_{1-x}S$ bulk crystal, as shown in Fig. 2.

Moreover, it is found that the TDOS peaks of $Mg_xZn_{1-x}S$ bulk crystal at around −4.5 eV are divided into two peaks with the increase of Mg dopant concentration, The TDOS peak of $Mg_{0.008}Zn_{0.992}S$ bulk crystal on the energy level of −4.0 eV is highest in $Mg_xZn_{1-x}S$ bulk crystal, and the TDOS peak of $Mg_xZn_{1-x}S$ bulk crystal near the VBM shifts downwards lower energy region, which also implies that the $Mg_{0.008}Zn_{0.992}S$ may be most stable in the Mg-doped, as shown in Table 1.

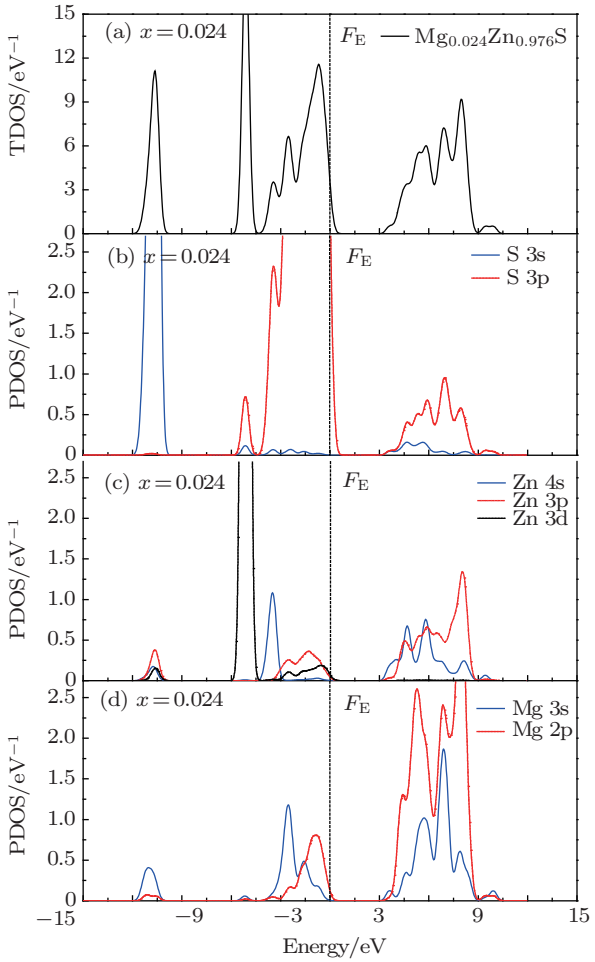


Fig. 7. (color online) Electronic densities of states for $Mg_{0.024}Zn_{0.976}S$.

3.3. Optical properties

In order to show the optical properties of $Mg_xZn_{1-x}S$ bulk crystal. The dielectric function and the optical absorption coefficient of $Mg_xZn_{1-x}S$ bulk crystal are calculated. The dielectric function and optical absorption coefficient are closely bound up with the electronic structure. Moreover, the dielectric function and optical absorption coefficient can be described by the complex dielectric function as[20]

$$\varepsilon(\omega) = \varepsilon_1(\omega) + i\varepsilon_2(\omega), \quad (1)$$

$$\varepsilon_1(\omega) = 1 + \frac{8\pi^2 e^2}{m^2} \cdot \sum_{V,C} \int_{BZ} d^3K \frac{2}{(2\pi)} \frac{|e \cdot M_{CV}(K)|^2}{[E_C(K) - E_V(K)]}, \quad (2)$$

$$\varepsilon_2(\omega) = \frac{4\pi^2}{m^2\omega^2}\cdot\sum_{V,C}\int_{\mathrm{BZ}} \mathrm{d}^3K\frac{2}{(2\pi)}\times|e\cdot M_{CV}(K)|^2, \times\delta\left[E_C(K)-E_V(K)-\hbar\omega\right], \quad (3)$$

$$\alpha(\omega) = \sqrt{2}\omega\left[\sqrt{\varepsilon_1^2(\omega)+\varepsilon_2^2(\omega)}-\varepsilon_1(\omega)\right]^{1/2}, \quad (4)$$

where $\alpha(\omega)$ is the optical absorption coefficient, $\varepsilon_1(\omega)$ and $\varepsilon_2(\omega)$ are the real part and imaginary part of the complex dielectric function $\varepsilon(\omega)$, respectively. The imaginary part $\varepsilon_2(\omega)$ is relevant to the band structure and the real part $\varepsilon_1(\omega)$ can be shown by the imaginary part $\varepsilon_2(\omega)$ in the form of Kramers-Kronig relation.

Figures 8 and 9 show the dielectric function spectra of real part $\varepsilon_1(\omega)$ and imaginary part $\varepsilon_2(\omega)$ for $Mg_xZn_{1-x}S$ bulk crystal, respectively. As shown in Fig. 8, the first dielectric absorption peak of real part $\varepsilon_1(\omega)$ for $Mg_xZn_{1-x}S$ bulk crystal at each value of x decreases and shifts upwards higher photon energy region with the increase of Mg-dopant concentration. Meanwhile, the zero frequency limits $\varepsilon_1(0)$, which relates to the dielectric response to the static electric field decreases from 6.2 to 4.4 as dopant composition x increases from 0 to 0.024, this leads to the increase of band gap for $Mg_xZn_{1-x}S$ bulk crystal in Fig. 2. In order to understand the dependence of dielectric function on band gap for $Mg_xZn_{1-x}S$ bulk crystal, the theoretical model[21] $\varepsilon_1(0)\approx 1+(\hbar\omega'/E_g)^2$ (ω' is the plasma frequency, $\hbar$ is the Dirac constant, and E_g is the band gap of $Mg_xZn_{1-x}S$ bulk crystal) clearly elucidates an inverse proportional relationship between the dielectric function and band gap of $Mg_xZn_{1-x}S$ bulk crystal.

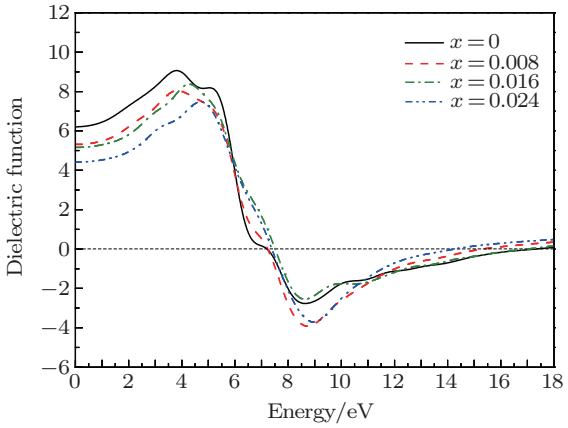


Fig. 8. (color online) Dielectric function spectra of real part for $Mg_xZn_{1-x}S$.

Figure 9 shows the imaginary part of the dielectric function for $Mg_xZn_{1-x}S$ bulk crystal. It is clear that the imaginary part $\varepsilon_2(\omega)$ of the dielectric function has a strong dielectric absorption region corresponding to incident photon energy range from 3.1 eV to 10 eV. In particular, the sharp dielectric absorption peaks in $\varepsilon_2(\omega)$ are found to be around 6.2 eV and 8 eV, which are mainly dominated by the S 3p electrons interacting with the Zn 4s electrons and Zn 3p electrons. The initial critical points of imaginary part $\varepsilon_2(\omega)$ for $Mg_xZn_{1-x}S$ bulk crystal are found to be around 0.11 eV, 0.54 eV, 1.12 eV, and 1.36 eV, respectively, which are also deemed to be the thresholds of the direct optical transitions occurring at 2.05 eV, 2.32 eV, 2.59 eV, and 2.91 eV for $Mg_xZn_{1-x}S$ bulk crystal, which corresponds to Mg-dopant composition x values of 0, 0.008, 0.016, and 0.024, respectively. Moreover, it is observed that for each of x values the first dielectric absorption peak of imaginary part $\varepsilon_2(\omega)$ occurs at around 6.2 eV decreases and the dielectric absorption peak of imaginary part $\varepsilon_2(\omega)$ shifts towards higher photon energy region with increasing the Mg-dopant composition, which validates the results that the band gap of $Mg_xZn_{1-x}S$ bulk crystal increases with the increase of Mg-dopant concentration in Fig. 2.

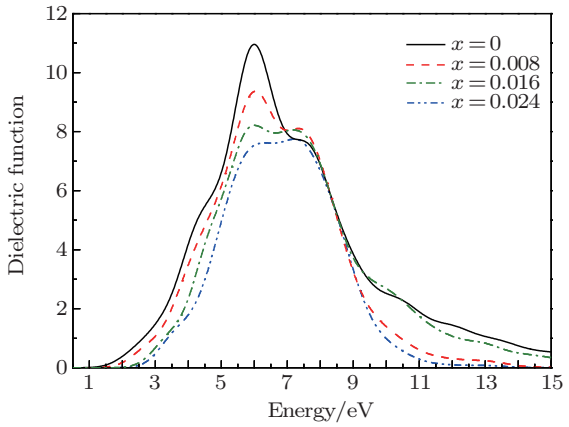


Fig. 9. (color online) Dielectric function spectra of imaginary part for $Mg_xZn_{1-x}S$.

Figure 10 shows the optical absorption spectra of $Mg_xZn_{1-x}S$ bulk crystal for some different values of x. It is observed that the optical absorption spectra of $Mg_xZn_{1-x}S$ bulk crystal are mainly displayed in the ultraviolet light region, which corresponds to photon wavelength ranging from 50 nm to 400 nm and the absorption coefficient maximum values of $Mg_xZn_{1-x}S$ bulk crystal are all higher than 2.75×10^5 cm^{-1}, which indicates the unique ultraviolet absorption properties and show an important potential application prospect for $Mg_xZn_{1-x}S$ bulk crystal in ultraviolet detectors. In particular, the optical absorption properties of $Mg_xZn_{1-x}S$ bulk crystal are improved when compared with those of pure ZnS bulk crystal, and the strongest absorption peaks are present in $Mg_{0.008}Zn_{0.992}S$ with the highest stability. Meanwhile, the optical absorption sides of $Mg_xZn_{1-x}S$ bulk crystal show an obvious blue shift with the increase of Mg doping concentration, which confirms the results that the band gap for $Mg_xZn_{1-x}S$ bulk crystal increases as Mg-dopant concentration increases (Fig. 2).

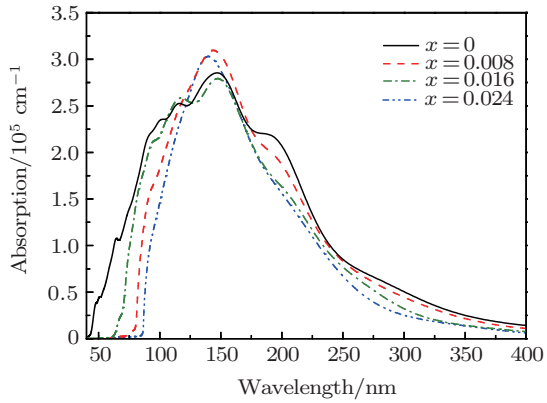


Fig. 10. (color online) Optical absorption spectra of $Mg_xZn_{1-x}S$.

4. Conclusions

In this paper, we determine the band structure, density of states, and optical properties of $Mg_xZn_{1-x}S$ bulk crystal using the first-principles calculations within the framework of density functional theory. The calculated results show that the $Mg_xZn_{1-x}S$ bulk crystal displays a direct band structure and the band gap increases from 2.05 eV to 2.91 eV as the Mg-doping concentration x increases from 0 to 0.024. In particular, the band gap of $Mg_xZn_{1-x}S$ bulk crystal can be evaluated by the first order function $E_g = 2.05 + 35.62x$, where dopant composition x ranges from 0 to 0.024. The top of the valence band is mainly dominated by the S 3p electrons, while the bottom of conduction band is mainly occupied by the Zn 4s electrons and Zn 3p electrons in $Mg_xZn_{1-x}S$ bulk crystal. Moreover, the dielectric constant decreases and the optical absorption peak shows an obvious blue shift. The results provide useful theoretical guidance for the potential application of $Mg_xZn_{1-x}S$ bulk crystals in optical detectors.

References

[1] Yu Y, Zhou J, Han H, Zhang C, Cai T, Song C and Gao T 2009 *J. Alloys Compd.* **471** 492
[2] Nistor S V, Stefan M, Nistor L C, Goovaerts E and Tendeloo G V 2010 *Phys. Rev. B* **81** 035336
[3] Tran T K, Park W, Tong W, Kyi M M, Wagner B K and Summers C J 1997 *J. Appl. Phys.* **81** 2803
[4] Fang X S, Wu L M and Hu L F 2011 *Adv. Mater.* **23** 585
[5] Moreau J W, Weber P K, Martin M C, Gilbert B, Hutcheon I D and Banfield J F 2007 *Science* **316** 1600
[6] Jiang Y, Meng X, Liu J, Xie Z, Lee C S and Lee S T 2003 *Adv. Mater.* **15** 323
[7] Li Y Q, Zapien J A, Shan Y Y, Liu Y K and Lee S T 2006 *Appl. Phys. Lett.* **88** 013115
[8] Hoa T T Q, The N D, Vitie S M, Nam N H, Vu L V, Canh T D and Long N N 2011 *Opt. Mater.* **33** 308
[9] Kim S, Lim T, Jung M, Kong K J, An K S and Ju S 2010 *J. Lumin.* **130** 2153
[10] Inoue R, Kitagawa M, Nishigaki T, Ichino K, Kobayashi H, Ohishi M and Saito H 1998 *J. Cryst. Growth* **184–185** 1076
[11] Chen Z, Li X X, Chen N, Du G P, Li Y S, Liu G H and Suen Y M 2012 *Mater. Sci. Eng. B* **177** 337
[12] Hu C E, Zeng Z Y, Cheng Y, Chen X R and Cai L C 2008 *Chin. Phys. B* **17** 3867
[13] Segall M D, Lindan P, Probert M J, Pickard C J, Hasnip P J, Clark S J and Payne M C 2002 *J. Phys.: Condens. Matter* **14** 2717
[14] Yu Z Q 2012 *Acta Phys. Sin.* **61** 217102 (in Chinese)
[15] Clark S J, Segall M D, Pickard C J, Hasnip P J, Probert M J, Refson K and Payne M C 2005 *Z. Kristallogr* **220** 567
[16] Perdew J, Burke K and Ernzerhof M 1996 *Phys. Rev. Lett.* **77** 3865
[17] Furdyna J K 1988 *J. Appl. Phys.* **64** 29
[18] Zhang J H, Ding J W, Cao J X and Zhang Y L 2011 *J. Solid State Chem.* **184** 477
[19] Ding J X, Zapien J A, Chen W W, Lifshitz Y, Lee S T and Meng X M 2004 *Appl. Phys. Lett.* **85** 2361
[20] Yu Z Q, Zhang C H and Lang J X 2014 *Acta Phys. Sin.* **63** 067102 (in Chinese)
[21] Penn D R 1962 *Phys. Rev.* **128** 2093